# Annotation-guided Protein Design with Multi-Level Domain Alignment

Chaohao Yuan[*]
Tsinghua University
Shenzhen, China
yuanch22@mails.tsinghua.edu.cn

Songyou Li
Renmin University of China
Beijing, China
songyou_li@126.com

Geyan Ye[†]
Tencent AI Lab
Shenzhen, China
blazerye@tencent.com

Yikun Zhang
Peking University
Shenzhen, China
yikun.zh@hotmail.com

Long-Kai Huang
Tencent AI Lab
Shenzhen, China
hlongkai@gmail.com

Wenbing Huang
Renmin University of China
Beijing, China
hwenbing@126.com

Wei Liu
Tencent AI Lab
Shenzhen, China
topliu@tencent.com

Jianhua Yao
Tencent AI Lab
Shenzhen, China
jianhua.yao@gmail.com

Yu Rong[‡]
DAMO Academy, Alibaba Group
Hangzhou, China
yu.rong@hotmail.com

## ABSTRACT

The core challenge of *de novo* protein design lies in creating proteins with specific functions or properties, guided by certain conditions. Current models explore to generate protein using structural and evolutionary guidance, which only provide indirect conditions concerning functions and properties. However, textual annotations of proteins, especially the annotations for protein domains, which directly describe the protein's high-level functionalities, properties, and their correlation with target amino acid sequences, remain unexplored in the context of protein design tasks. In this paper, we propose **P**rotein-**A**nnotation **A**lignment **G**eneration (PAAG), a multi-modality protein design framework that integrates the textual annotations extracted from protein database for controllable generation in sequence space. Specifically, within a multi-level alignment module, PAAG can explicitly generate proteins containing specific domains conditioned on the corresponding domain annotations, and can even design novel proteins with flexible combinations of different kinds of annotations. Our experimental results underscore the superiority of the aligned protein representations from PAAG over 7 prediction tasks. Furthermore, PAAG demonstrates a significant increase in generation success rate (24.7% vs 4.7% in zinc finger, and 54.3% vs 22.0% in the immunoglobulin domain) in comparison to the existing model. We anticipate that PAAG will broaden the horizons of protein design by leveraging the knowledge from between textual annotation and proteins.

## CCS CONCEPTS

• **Applied computing → Computational biology**.

## KEYWORDS

Annotation-guided protein design, multi-modality alignment

**ACM Reference Format:**
Chaohao Yuan, Songyou Li, Geyan Ye, Yikun Zhang, Long-Kai Huang, Wenbing Huang, Wei Liu, Jianhua Yao, and Yu Rong. 2018. Annotation-guided Protein Design with Multi-Level Domain Alignment. In *Proceedings of Make sure to enter the correct conference title from your rights confirmation emai (Conference acronym 'XX)*. ACM, New York, NY, USA, 12 pages. https://doi.org/XXXXXXX.XXXXXXX

## 1 INTRODUCTION

Protein design [33] is a crucial task for its immense potential on drug discovery [44, 52], enzyme engineering [47], immunongineering [48] and so on. The generation of proteins with specific properties, behaviors, or functions, such as optimizing the binding affinity to given molecules [18, 60] or incorporating a particular ion-binding site [39], is known as *de novo* protein design. This process presents a significant challenge due to the vast space of protein sequences and the complexity of protein functions. Recently, machine learning models have shown profound potential for protein design. The existing studies mostly rely on the structural [51] or evolutionary information [1] as the guidance to design proteins. However, in many cases, these conditions can only offer indirect guidance towards the desired protein design targets to their inherent ambiguity. For example, the same protein sequence segment can be either act as receptors to regulate synaptic function [45] or helpers to locate target proteins to specific subcellular locations [35].

In addition to the structural and evolutionary information, the current protein dataset, such as Swiss-Prot [5] and UniProtKB [9],

[*] Work was done when Chaohao Yuan worked as an intern at Tencent AI Lab.
[†] Project Lead.
[‡] Corresponding Author.

*Conference acronym 'XX, June 03–05, 2018, Woodstock, NY*

ACM ISBN 978-1-4503-XXXX-X/18/06
https://doi.org/XXXXXXX.XXXXXXX

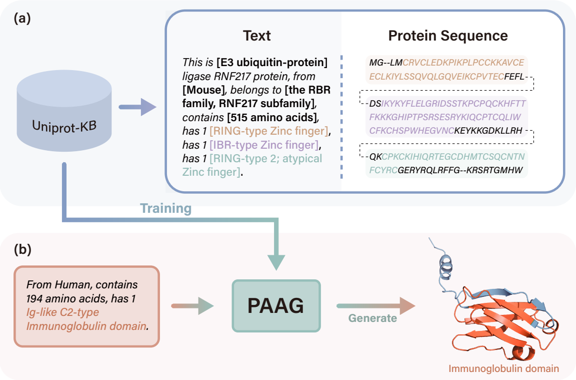
(a)
Uniprot-KB
Text
Protein Sequence
This is [E3 ubiquitin-protein] ligase RNF217 protein, from [Mouse], belongs to [the RBR family, RNF217 subfamily], contains [515 amino acids], has 1 [RING-type Zinc finger], has 1 [IBR-type Zinc finger], has 1 [RING-type 2; atypical Zinc finger].
MG--LMCRVCLEDKPIKPLPCCKKAVCE
ECLKIYLSSQVQLGQVEIKCPVTECFEFL-
-DSIKYKYFLELGRIDSSTKPCPQCKHFTT
FKKKGHIPTPSRSESRYKIQCPTCQLIW
CFKCHSPWHEGVNCKEYKKGDKLLRH-
-QKCPKCKIHIQRTEGCDHMTCSQCNTN
FCYRCGERYRQLRFFG--KRSRTGMHW
Training
(b)
From Human, contains 194 amino acids, has 1 Ig-like C2-type Immunoglobulin domain.
PAAG
Generate
Immunoglobulin domain

**Figure 1: (a) The example of property annotations (in bold) and domain annotations (in colors). (b). The illustration of annotation-guided protein design with PAAG. Given the input of textual description within immunoglobulin domain annotation, PAAG can generate the proteins containing immunoglobulin domain.**

contains rich textual annotations derived from wet laboratory experiments and literature. Figure 1 illustrates an example of the textual annotations on the zinc-finger protein. Generally, these annotations can be categorized into *property annotation* and *domain annotation*. *Property annotation* represents a piece of text that depicts the global property of proteins, such as protein names, number of amino acids, subcellular localization [3] and thermostability [11]. Conversely, *domain annotation* pertains to the knowledge derived from the local domain [13] of proteins, which is a subregion of amino acid sequence that is self-stabilizing and represents certain structural and functional aspects of the protein. These annotations provide both coarse and fine-grained information regarding protein’s functions, properties, and interactions, thereby encompassing knowledge with the potential to guide the generation and design of novel proteins.

For instance, as one of crucial functional domains of DNA/RNA binding proteins [8], the zinc-finger domain naturally has many variants, such as C2H2 type, CCHC type and Zinc ribbon type. These variants exhibit significant differences in both structural and evolutionary features among them which is hard covered by structural and evolutionary conditions. On the contrary, the “zinc-finger” annotation from the protein database inherently provides a more effective means of describing the high-level knowledge span across both sequences and structures. Hence, we aim to investigate the following question: *Is it possible to leverage such textual annotations to guide the delicate controllable protein design?*

Recently, several primary attempts have been made to leverage such textual annotations to guide the protein generation. Examples include training an individual protein caption model to guide the diffusion generation process [21], and incorporating the an overall text description through a global language-to-protein alignment model [31]. However, current models cannot flexibly combine the different conditions and lack of the capability for fine-grained control, such as specifying the generation of particular domains.

To fill these gaps, in this paper, we introduce a novel framework, **P**rotein-**A**nnotation **A**lignment **G**eneration(PAAG), that enables annotation-guided protein design by aligning protein sequences with their textual annotations. Specifically, we first consider both property and domain annotations in proteins and design a multi-level alignment module to align the representations of sequences and annotations extracted from the existing encoders in both global and local level. For the generation task, PAAG utilizes an autoregressive decoder to generate protein sequences guided by the aligned representation of textual annotations. Additionally, PAAG employs an end-to-end training pipeline that joint training of alignment and generation tasks without freezing the parameters in sequence and text encoders. This joint training enhances the understanding of the complex and flexible annotation condition, resulting in improved guided generation. Figure 1 demonstrates an example of annotation-guided generation. In experiments, we first investigate the quality of protein representations from PAAG by seven predictive downstream tasks. PAAG surpasses state-of-the-art baseline with an average relative improvement of 1.5%. Subsequently, three protein generation tasks are conducted to assess the capabilities of PAAG. In the case of unconditional generation, PAAG produces sequences exhibiting the highest degree of novelty while maintaining the distribution of natural proteins. For the two conditional protein design tasks, PAAG demonstrates a nearly threefold increase in generation success rate (24.7% vs 4.7% in zinc finger, and 54.3% vs 22.0% in the immunoglobulin domain)[1] in comparison to the existing model. Our contributions are summarized as follows:

- We propose the first annotation-guided protein design paradigm, integrating local and global annotation information. Our proposed framework PAAG is the first approach that can generate proteins containing specific domains, guided by their corresponding annotations with high success rate.
- PAAG features a multi-level alignment module for handling annotation and protein data alignment at various granularities. Joint training of alignment and generation tasks allows the model to produce improved protein representations, consequently boosting performance in predictive and generative tasks.
- Comprehensive experiments on 7 predictive and 3 generative tasks showcase PAAG’s superiority compared to the existing methods. Notably, PAAG is not only capable of generating proteins that include a single annotation, but it also successfully generates proteins adhering to the flexible conditions of multiple annotation combinations.

# 2 PRELIMINARIES

## 2.1 Protein and Its Textual Annotations

The primary structure of a protein can be represented as an amino acid sequence $S = (s_1, s_2, \cdots, s_n)$, where $s_i$ is the $i$-th amino acids chosen from 20 different amino acids which are represented as 20 characters. Given a protein $S$, the annotation-sequence pair set $\mathcal{D}_S = \{(T_k, S^k_{i:j})\}_{k=1}^{K_S}$ is constructed by extracting the correspondence between textual annotations and protein domains & properties from protein database, such as UniProtKB [9], where $T_k$ is the textual annotations of the $k$-th domain $S^k_{i:j}$ of the protein and $K_S$ is the number of annotation-domain pairs of the protein $S$. For the property annotation, the corresponding domain is the entire sequence, i.e, $S_{1:|S|}$. This annotation-domain pair set $\mathcal{D}_S$ provides

[1] This is the success rate with quality threshold $e = 1$, i.e., $\mathrm{SR}_1$.

comprehensive knowledge about the protein $S$ and, therefore, plays an important role in training the protein generation model.

## 2.2 Encoders for Proteins and Annotations

We adopt a protein encoder (PE) to generate both the protein and its domain representations based on the amino acid sequence as $z_S = f_{\text{PE}}(S)$, where $f_{\text{PE}}$ is the protein encoder and $z_S$ is the embedding of $S$. For textual annotations, we generate their representations using the pre-trained language model $f_{\text{LM}}$ as $z_{\mathcal{A}_S} = f_{\text{LM}}(G(\mathcal{A}_S))$, where $\mathcal{A}_S \subseteq \{T_k | (T_k, S^k_{i:j}) \in \mathcal{D}_S\}$ is a subset of the annotations in the annotation-domain pair set for a protein $S$, $G()$ is a template function which converts a set of annotations to a textual description, the details of $G()$ can be found in Appendix A.2, and $z_{\mathcal{A}}$ is the embedding of the annotation set. Note that the annotation subset can cover all annotations in $\mathcal{D}_S$ or just one. If $\mathcal{A}_S$ covers only one annotation $T_0$, we can skip the template function and directly generate the embedding of $T_0$ using $f_{\text{LM}}$.

We employ transformer-based protein encoder and text encoder as our base model and initialize them with pre-trained models. Specifically, we employ SciBERT[6], which is pre-trained on computer science and biological datasets, to initialize the text encoder $f_{\text{LM}}$. The pre-trained protein encoder, ProtBERT[14], is used to initialize the protein encoder $f_{\text{PE}}$.

# 3 METHODOLOGY

In this section, we propose a novel framework, **P**rotein-**A**nnotation **A**lignment **G**eneration(PAAG), which enables the flexible annotations-guided protein design. Figure 2 illustrates the overall framework of PAAG. In the following, we present the details of each component of PAAG.

## 3.1 Multi-level Protein and Annotation Alignment

We will first employ template function $G$ to translate these annotations as textual descriptions and then utilize a language model to extract the representation of the annotation set $z_{\mathcal{A}} = f_{\text{LM}}(G(\mathcal{A}))$. Then the protein sequence is generated using a decoder $f_D$ based on this representation as $S = f_{\text{D}}(z_{\mathcal{A}})$.

To better integrate the information between proteins and annotations, we aim to align the multi-level representations of proteins and annotations. Specifically, we conduct local alignment and global alignment by performing contrastive learning at domain level and protein level, respectively.

We measure the alignment score using the cosine similarity between the embeddings of protein and the annotation set, which is defined as

$$s(\mathcal{A}, S) = \frac{\langle \text{Proj}_{\mathcal{A}}(z_{\mathcal{A}}), \text{Proj}_S(z_S) \rangle}{\|\text{Proj}_{\mathcal{A}}(z_{\mathcal{A}})\| \|\text{Proj}_S(z_S)\|}, \tag{1}$$

where $\text{Proj}_a(z) = \boldsymbol{W}_a \boldsymbol{z} + \boldsymbol{b}$ projects the input $\boldsymbol{z}$ into a latent space with dimension $h$. $\boldsymbol{W}_a \in \mathbb{R}^{h \times |\boldsymbol{z}|}$ and $\boldsymbol{b} \in \mathbb{R}^h$ are trainable parameters. During alignment, we encourage the matched (positive) pairs to have representations with higher similarity $s$ than unmatched (negative) pairs. We next will explain in detail how to construct the positive and negative pairs in our multi-level framework.

### 3.1.1 *Local Alignment.*

Given a protein $S$, and its annotation-domain pairs set $\mathcal{D}_S$, in domain-level, we aim to align the representation of the domain $S^k_{i:j}$ and its corresponding annotation $T_k$ and use all annotation-domain pairs in $\mathcal{D}_S$ as positive pair. To construct the negative pairs, we randomly sample the sub-regions outside the domain $S^k_{i:j}$, i.e. $S^k_{1:i-1} \cup S^k_{j+1:l}$, as the negative samples $S^{k-}_{i:j}$ of the domain.

**Annotation-Domain Contrastive(ADC) Loss:** In designing this loss, since our objective is on identifying functional regions within proteins, we consider amino acid sequences from the same protein as negative samples. Specifically, we adopt InfoNCE loss as the ADC loss to align the representations of local annotation $z_T$ and functional domain $z_{S_{i:j}}$ as

$$\mathcal{L}_{\text{ADC}} = -\frac{1}{K_S} \sum_{k=1}^{K_S} \log \frac{\exp(s(T_k, S^k_{i:j})/\tau)}{\sum_{n=1}^{N} \exp(s(T_n, S^{n-}_{i:j})/\tau)}, \tag{2}$$

where $K_S$ is the number of functional domains for the protein $S$, $N$ is the number of negative samples, and $\tau$ is a learnable temperature parameter.

The local alignment enables PAAG to explicitly learn the relation between the functional domain and its annotation. Therefore, we can use the model to controllably generate the specific functional domain given annotations.

### 3.1.2 *Global Alignment.*

To enable global alignment, we utilize template function $G(\cdot)$ to construct protein-level textual description and form the positive protein-description pairs as $\{(G(\mathcal{A}_S), S)\}$. Since multiple annotations and the entire protein will be more complex, to enlarge the number of negative samples for global alignment, we follow the setting of MOCO [17] to construct momentum encoders $f_m$ as:

$$f_m \leftarrow m f_m + (1 - m) f. \tag{3}$$

where the encoder $f$ can be either protein encoder $f_{\text{PE}}$ or text encoder $f_{\text{LM}}$, and $m$ is the momentum hyperparameter. We follow implementation details in [27] and [26] to construct the momentum encoders for both encoders. The momentum encoders extract consistent features to increase the number of negative samples, and the dynamic dictionaries will store these features.

**Annotation-Protein Contrastive (APC) Loss** is designed to align the representations of global properties $z_{\mathcal{A}}$ with protein $z_S$. Specifically, for each protein sequence and annotation set, we calculate the softmax-normalized sequence-to-annotation and annotation-to-sequence similarity as:

$$p^{\text{s2a}}_m(S) = \frac{\exp(s(A_m, S)/\tau)}{\sum_{m=1}^{M} \exp(s(A_m, S)/\tau)}, \tag{4}$$

$$p^{\text{a2s}}_m(A) = \frac{\exp(s(A, S_m)/\tau)}{\sum_{m=1}^{M} \exp(s(A, S_m)/\tau)}, \tag{5}$$

where $\tau$ is a learnable temperature parameter, $A_m$ and $S_m$ indicate their representations will be extracted by respective momentum encoders.

Denote $\vec{y}^{\text{ a2s}}(A)$ and $\vec{y}^{\text{ s2a}}(S)$ as the ground-truth one-hot similarity, where negative pairs have a probability of 0 and the positive pair has a probability of 1. The annotation-protein contrastive loss is defined as the cross-entropy H between $\vec{p}$ and $\vec{y}$:

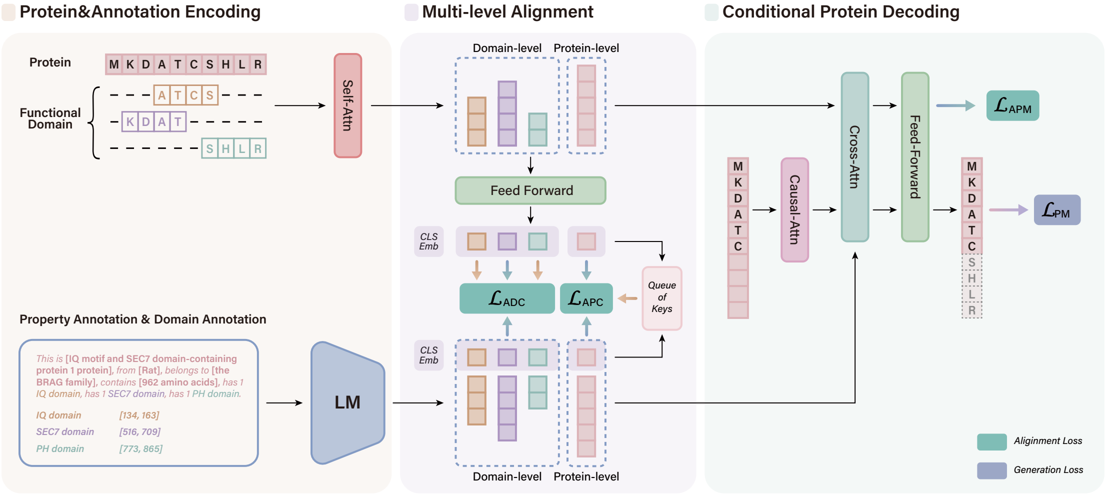
Protein&Annotation Encoding
Multi-level Alignment
Conditional Protein Decoding
Protein
M K D A T C S H L R
Functional Domain
A T C S
K D A T
S H L R
Self-Attn
Domain-level
Protein-level
Feed Forward
CLS Emb
$\mathcal{L}_{\text{ADC}}$
$\mathcal{L}_{\text{APC}}$
Queue of Keys
CLS Emb
Domain-level
Protein-level
Property Annotation & Domain Annotation
This is [IQ motif and SEC7 domain-containing protein 1 protein], from [Rat], belongs to [the BRAG family], contains [962 amino acids], has 1 IQ domain, has 1 SEC7 domain, has 1 PH domain.
IQ domain [134, 163]
SEC7 domain [516, 709]
PH domain [773, 865]
LM
M K D A T C
Causal-Attn
Cross-Attn
Feed-Forward
$\mathcal{L}_{\text{APM}}$
M K D A T C S H L R
$\mathcal{L}_{\text{PM}}$
Alignment Loss
Generation Loss

**Figure 2: The overall framework of PAAG. The same parameters share the same color. PAAG contains three modules. (1) Protein & Annotation Encoding module encode the input protein sequence & domains and corresponding annotations to the embeddings. (2) Multi-level alignment module projects the protein and annotation embeddings into and employs Annotation-Protein Contrasive (APC) loss, Annotation-Domain Contrasive (ADC) loss and Annotation-Protein Matching (APM) loss to align them in a same latent space. (3) Conditional Protein Decoding accepts the annotation embedding as input and generate the protein sequence.**

$$\begin{aligned}\mathcal{L}_{\text{APC}} = \frac{1}{2}\mathbb{E}_{(S,A)\sim D}\big[&\text{H}(\vec{y}^{\text{ s2a}}(S), \vec{p}^{\text{ s2a}}(S)) \\ &+\text{H}(\vec{y}^{\text{ a2s}}(A), \vec{p}^{\text{ a2s}}(A))\big]\end{aligned}. \tag{6}$$

Through APC loss, PAAG aligns the representations of two modalities, improving the quality of aligned representation, which is crucial for downstream tasks such as classification and regression.

**Annotation-Protein Matching (APM) Loss**. Inspired by [26], we introduce a multi-modal encoder $f_{\text{ME}}$, which integrates the representation of annotations and protein as $z^M_{S,\mathcal{A}} = f_{\text{ME}}(S, G(\mathcal{A}))$, to identify whether the given pairs of protein description $G(\mathcal{A})$ and protein $S$ are matched or not. Specially, the multimodal encoder $f_{\text{ME}}$ is transformer-based and shares the parameters of self-attention and feed-forward layers with $f_{\text{PE}}$ and has additional cross-attention layers between self-attention layers and feed-forward layers to integrate the text information. The cross-attention layers share the same cross-attention parameters as the decoder.

Annotation-Protein Matching (APM) Loss aims to facilitate the learning of multimodal representations. Additionally, we use the hard negative strategy, where we first select the most similar negative pairs and then use these most challenging negative pairs to optimize the model through in the training of the model with the APM loss, enabling the encoder to learn informative representations. To construct the APM loss, we extract the multi-modal representation as $z^M_{S,\mathcal{A}} = f_{\text{ME}}(S, G(\mathcal{A}))$ and use a classifier to classify its probability of being positive or negative, which is denoted by $\vec{p}^{\text{APM}}(\mathcal{A}, S)$. And we compute the cross-entropy between the ground-truth label $\vec{y}^{\text{APM}}(A, S)$ indicating the protein-description pair being positive or negative to obtain the APM loss as

$$\mathcal{L}_{\text{APM}} = \mathbb{E}_{(A,S)}\text{H}(\vec{y}^{\text{APM}}(A, S), \vec{p}^{\text{APM}}(A, S)). \tag{7}$$

APM loss trains the cross-attention layers for integrating two modalities. These cross-attention will be shared with protein decoder, which helps protein decoder interpret textual information. In Sec. 4.7, we demonstrate the importance of APM loss.

## 3.2 Conditional Protein Decoding

**Protein Decoder.** Our ultimate goal is generating functional proteins conditioned on a set of annotations $\mathcal{A} = \{T_k\}_{k=1}^K$. We adopt an auto-regressive protein decoder $f_{\text{D}}$ that can receive the condition from the language model. Specifically, the decoder will first process the protein sequence through causal attention layers to enable auto-regressive generation, then integrate the information from annotations via cross-attention layers followed by feed-forward layers. Note that the causal attention layers are initialized using the same weights as the self-attention layers in the protein encoder and the feed-forward layers share the same parameters as the protein encoder. Here, the parameter-sharing mechanism enables higher training efficiency [25]. The cross-attention layers are randomly initialized and trained from scratch.

**Protein Modeling (PM) Loss**. To guide the learning of the model, we estimate the PM loss as

$$\mathcal{L}_{PM} = -\sum_{i=1}^{l} \log p(S_i|S_{<i}; \mathcal{A}), \tag{8}$$

where $l$ is the length of the protein $S$ and $p(S_i|S_{<i}; \mathcal{A})$ is the predicted probability of the $i$-th amino acid given all previous amino acids and the annotation set.

## 3.3 Training Objectives

In the training of PAAG, we optimize four objective functions. These functions are designed to align the representations between annotations and protein sequences, integrate the two modalities, and reconstruct the protein sequence. In contrast to ProteinDT [29], which splits the training process into three separate stages, PAAG jointly optimizes these four objective functions in an end-to-end manner. The overall pretraining objective of PAAG is :

$$\mathcal{L} = \mathcal{L}_{\text{ADC}} + \mathcal{L}_{\text{APC}} + \mathcal{L}_{\text{APM}} + \mathcal{L}_{\text{PM}}. \tag{9}$$

## 3.4 Annotation-guided Protein Design

After obtaining the model $F$ of PAAG, we can use $F$ to design the proteins with given textual annotations. In the following, we given the definition of annotation-guided protein design.

**Definition 3.1** (Annotation-guided Protein Design). Given an annotation set $\mathcal{A} = \{T_k\}_{k=1}^{K}$ with $K$ annotations, a generative model $F$ can leverage the information from $\{T_k\}_{k=1}^{K}$ to generate the protein $S$ which satisfies the condition described in $\{T_k\}_{k=1}^{K}$. Quantitatively, this task aims to maximize the following objective function:

$$\max \sum_{T \in \mathcal{A}} \mathrm{M}_T(S), \text{ s.t. } S = F(\mathcal{A}), \tag{10}$$

where $\mathrm{M}_T(\cdot)$ is metric function for the annotation $T$.

In this paper, we mainly focus on two type of metrics, *functional-domain metric* and *global-property metric*.

- **Functional-domain metric**: for the annotation describing a certain functional domain, $\mathrm{M}_T()$ will invoke a profile hidden Markov models from Pfam [34] to search for the optimal match within protein $S$ regarding to the domain described by annotation $T$ and assign an e-value $s$ to this match. Given an e-value threshold $e$, we have:

  $$\mathrm{M}_{T,e}(S) = \mathbb{1}_S(s < e), \tag{11}$$

  where $\mathbb{1}_S(\text{cond})$ outputs 1 when cond = True, otherwise, outputs 0.
- **Global-property metric**: for the annotations describing protein's global properties, $\mathrm{M}_T()$ employ a pre-defined oracle to determine if the given $S$ has the property described by the annotation $T$ and output a score $s$ in the range of $[0, 1]$. Here, 0 denotes the absence of the property, while 1 signifies its presence.

# 4 EXPERIMENT

In this section, we extensively evaluate PAAG from two aspects: (1). quality of aligned protein representation for the predictive tasks; (2) evaluation on the unconditional sequence generation and protein design with textual annotations.

## 4.1 Construction of ProtAnnotation Dataset

To enable multi-level alignment, we build the ProtAnnotation dataset with annotation-sequence pair set for protein design task. Specifically, we select the proteins with "Domain" entry in UniProtKB [9] to build ProtAnnotation dataset.

However, since the biases within our training dataset will significantly impact the performance of PAAG, we limit our selection to protein-annotation pairs from a refined subset of UniProtKB, namely Swiss-Prot. Each entry in Swiss-Prot has been manually reviewed and supplemented with detailed information with protein function, structure, and interactions. Ultimately, the ProtAnnotation consists of 129,727 proteins. Moreover, in our alignment, we incorporate temperature [54] to control the similarity scores of distribution between positive and negative pairs. An appropriate temperature can soften these scores, making the model less sensitive to noisy samples. This adaptability allows the learning process to focus more on meaningful correlations and reduce the impact of irrelevant variations, ultimately enhancing the PAAG's robustness.

The domain annotations are extracted by these "Domain" entries including the domain description and start & end index of this domain. Additionally, we select four properties as the property annotations, that is, "protein_name", "organism_name", "length" and "SIMLARITY". The textual description is assembled by the template function $G$, which can accept any subset of annotation as input. More details, including the data examples are deferred in Appendix A.2.

## 4.2 Quality of Aligned Representation

We first conduct multiple experiments on predictive tasks, to evaluate the quality of protein representation produced by PAAG.

**Settings:** To make a fair comparison with ProtST, we use the same proteins in dataset ProtDescribe [56] to first pretrain PAAG, followed by full-model fine-tuning on various downstream tasks. For the full-model fine-tuning, we add a task head for each task and fine-tune the model for 100 epochs. We use the validation set to select the model and report the results on random seed 0, adhering to the same settings as in ProtST [56]. More details are deferred in Appendix A.6.

**Benchmark Tasks:** We adopt 7 downstream tasks within two task types as the benchmark task.

- **Protein Localization Prediction** aims to forecast the subcellular locations of proteins. Derived from DeepLoc [3], we focus on two similar tasks. The subcellular localization prediction (*Abbr. as*, Sub) encompasses 10 location categories and binary localization prediction (*Abbr. as*, Bin) that includes 2 location categories, soluble and membrane-bound. The splits of data follow the original split in DeepLoc.
- **Fitness Landscape Prediction** is primarily focused on the prediction of the effects of residue mutations on the fitness of proteins. We evaluate our models on $\beta$-lactamase (*Abbr.*, $\beta$-lac) landscape from PEER [57], the AAV and Thermostability (*Abbr.*, Thermo) landscapes from FLIP [11], and the Fluorescence (*Abbr.*, Flu) and Stability (*Abbr.*, Sta) landscapes from TAPE [38]. The splits of data follow the splitting setting of ProtST [56]

**Baselines:** We adopt two types of baseline. The first type is the models trained from scratch, including CNN [41], ResNet [38], LSTM [38], Transformer [38]. The second type is the pre-trained models with full model tuning, including OntoProtein [58], ProtBert [14] and ESM2 [28]. For the ProtST and PAAG, we train two variants with different initialization weights from ProtBert and ESM2 to verify the enhancement of text knowledge on protein representations from different protein encoders. We utilize distinct subscripts to denote the initialized parameters, such as $\text{PAAG}_{\text{ProtBert}}$ and $\text{PAAG}_{\text{ESM2}}$.

**Results:** Table 1 reports the results of all models on seven baselines. As illustrated in Table 1, PAAG achieves superior performance in comparison to the baselines on all 7 tasks. These results highlight the robust generalization capabilities of PAAG for downstream tasks. Specifically, PAAG outperforms the vanilla pretrained models, ProtBert and ESM2, in all cases, indicating that PAAG can further enhance the quality of protein representation by incorporating the knowledge from textual annotations. According to the results in Table 1, multi-modal training has a positive influence on the performance of downstream tasks in both ProtST and PAAG. Additionally,

**Table 1: Results on protein localization prediction and protein landscape prediction benchmarks. Bold in green and underlined numbers indicate the best and the second best result, respectively.**

| Model | **Loc. pred.** (Acc%) | | **Fitness pred.** (Spearman's $\rho$) | | | | |
|---|---|---|---|---|---|---|---|
| | **Bin** ↑ | **Sub** ↑ | $\rho$**-lac** ↑ | **AAV** ↑ | **Thermo** ↑ | **Flu** ↑ | **Sta** ↑ |
| **Models trained from scratch** | | | | | | | |
| **CNN** | 82.67 | 58.73 | 0.781 | 0.746 | 0.494 | **0.682** | 0.637 |
| **ResNet** | 78.99 | 52.30 | 0.152 | 0.739 | 0.528 | 0.636 | 0.126 |
| **LSTM** | 88.11 | 62.98 | 0.139 | 0.125 | 0.564 | 0.494 | 0.533 |
| **Transformer** | 75.74 | 56.02 | 0.261 | 0.681 | 0.545 | 0.643 | 0.649 |
| **Models with full model tuning** | | | | | | | |
| **OntoProtein** | 92.47 | 77.59 | 0.757 | 0.791 | 0.662 | 0.630 | 0.731 |
| **ProtBert** | 91.32 | 76.53 | 0.731 | 0.794 | 0.660 | 0.679 | 0.771 |
| **ESM2** | 91.72 | 78.67 | 0.867 | 0.817 | 0.672 | 0.677 | 0.718 |
| **ProtST**$_{\text{ProtBert}}$ | 91.78 | 78.71 | 0.863 | 0.804 | 0.673 | 0.679 | 0.745 |
| **ProtST**$_{\text{ESM2}}$ | 92.52 | 80.22 | 0.879 | 0.825 | 0.682 | **0.682** | 0.738 |
| **PAAG**$_{\text{ProtBert}}$ | **92.63** | 78.96 | 0.820 | 0.825 | 0.668 | 0.680 | **0.788** |
| **PAAG**$_{\text{ESM2}}$ | 92.46 | **81.30** | **0.888** | **0.839** | **0.684** | **0.682** | 0.737 |

the performance improvement of PAAG surpasses that of ProtST in 10 out of 14 cases, further validating the effectiveness of PAAG in augmenting the quality of protein representation.

## 4.3 Unconditional Protein Generation

To verify the learning effect of the decoder, we compare the ability of different models in unconditional generation task. A good decoder is able to generate protein sequences that conform to the distribution of the training set while simultaneously exhibiting adequate novelty.

**Setting:** In unconditional generation task, we only specify the length of generated proteins and conditions. We sample the same length from natural proteins, to ensue a fair comparisons across different models.

**Baselines:** We compare PAAG with 3 representative protein design models, *i.e.*, ProGen [32], Chroma [21] and ProteinDT [31]. Furthermore, we introduce two naive baselines: Random$_{\text{Uniform}}$ and Random$_{\text{Empirical}}$. Random$_{\text{Uniform}}$ generates protein sequence by randomly selecting amino acids based on a uniform distribution, while Random$_{\text{Empirical}}$ adheres to the empirical amino acid distribution in the training dataset. Additionally, we report the results of the sequence set sampled from natural proteins, denoted as Natural, to serve as a reference. The details of baselines are in Appendix A.5.

**Evaluation metrics:** To evaluate the quality of generated protein sequences, we employ three metrics: Distinct-n, Diversity and Novelty. Suppose $\mathcal{S}$ is the protein sequence set.

- **Distinct-n** [24] is a classical metric in natural language processing that measures textual diversity of generated text by counting distinct n-grams. We use normalized Distinct-n to assess the fraction of repetitive sequence motifs in sequences from $\mathcal{S}$, which exhibits the biological importance [4]. A higher Distinct-n suggests fewer repetitive amino acid segments. We set $n = 2$ here.
- **Diversity** measures the dissimilarity of sequences in $\mathcal{S}$. We employ Mmseq2 [46] to compute the dissimilarity between each pair of sequences, and utilize the mean of these dissimilarities as Diversity. A higher Diversity signifies a greater diversity in $\mathcal{S}$.
- **Novelty** measures the novelty of sequences in $\mathcal{S}$ compared to a reference set. We take UniprotKB [9] as the reference set. For each sequences in $\mathcal{S}$, we employ Mmseq2 [46] to return the dissimilarity score of the most similar sequence in UniprotKB. Novelty is defined as the mean of dissimilarity score for all sequences in $\mathcal{S}$. A higher Novelty indicates the generated sequences exhibit substantial novelty comparing with the reference set.

**Table 2: Results of the unconditional generation task. The values in parentheses Δ% represent the absolute relative difference from the values of Natural.**

| **Model** | **Distinct-2** (Δ%) | **Diversity**(Δ%) | **Novelty** ↑ |
|---|---|---|---|
| **Natural** | 0.4309(0) | 0.829(0) | - |
| **Random**$_{\text{Uniform}}$ | 0.5006(16.18%) | 0.847(2.17%) | 0.713 |
| **Random**$_{\text{Empirical}}$ | 0.4442(3.09%) | 0.834(**0.60%**) | 0.721 |
| **ProGEN** | 0.3003(30.31%) | 0.845(1.93%) | 0.374 |
| **Chroma** | 0.3211(25.48%) | 0.855(3.14%) | 0.638 |
| **ProteinDT** | 0.4909(13.92%) | 0.814(1.81%) | 0.578 |
| **PAAG** | 0.4314(**0.12%**) | 0.815(1.69%) | **0.766** |

**Results:** Table 2 shows the results of unconditional generation under three metrics. From Table 2, we can observe that:

- PAAG achieves the highest novelty, indicating PAAG captures the intrinsic relationship between amino acids, rather than merely memorizing protein sequences in the training set.
- PAAG exhibits the closest Distince-n score compared with natural proteins, which proves that proteins generated by PAAG possess similar amino acid distribution as natural proteins.
- Since Random$_{\text{Empirical}}$ generates protein sequence following the empirical amino acid distribution in the natural proteins, it is reasonable to obtain the closest diversity to natural proteins. Compared with other learning-based model, PAAG still maintains the closest diversity to natural proteins proving PAAG has the similar distribution at protein level.
- ProGen and Chroma have considerably lower Distince-n score in comparison to PAAG and natural proteins, implying an abundance of repetitions within generated protein sequence. While ProteinDT has higher Distince-n score, it also fails to capture the intrinsic amino acid distrbution in natrual proteins.

In a summary, PAAG is capable of generating high-quality protein sequences, aided by the the multi-level alignment process.

## 4.4 Protein Design with Domain Annotations

In this section, we evaluate the performance of PAAG in generating proteins under the given domain annotations.

**Settings:** We utilize two biologically significant domains, zinc-finger domain [23] and immunoglobulin domain [7], as the target domain annotation to generate the proteins respectively. For each case, we generate $N = 300$ protein sequences given the length of the proteins and the annotation set containing the domain annotations of "zinc-finger" or "immunoglobulin domain". For all models, the protein sequences are generated with the same length sampled from natural proteins that have corresponding domain in UniprotKB. To further evaluate the generalization ability of PAAG, we further test our model on generating proteins with EGF-like domain. The details can be found in Appendix A.7.1.

Based on (11), we further define a metric: success rate $\text{SR}_e = \frac{M_{T,e}(S)}{N}$ to measure the generation quality with the proportion of proteins that successfully identify the specific domain with the quality threshold $e$.

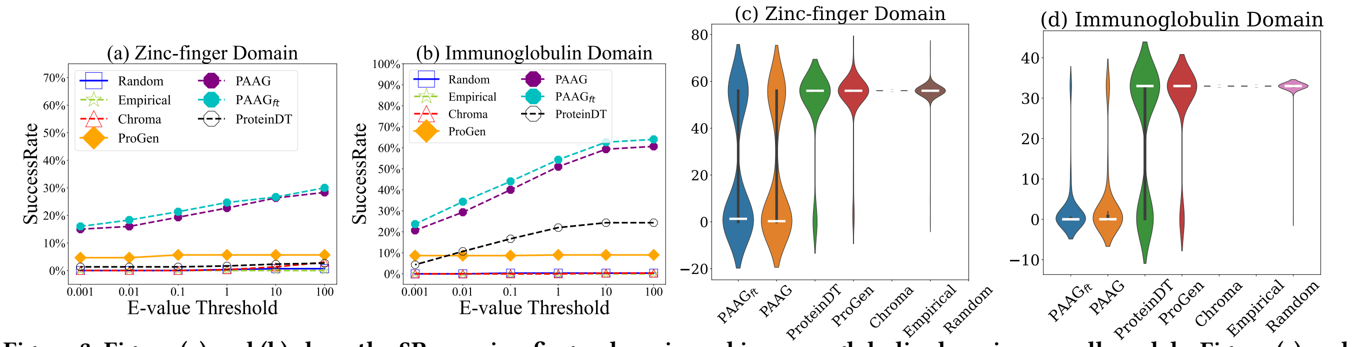

**Figure 3: Figure (a) and (b) show the SR$_e$ on zinc-finger domain and immunoglobulin domain over all models. Figure (c) and (d) show their distributions of e-value. White bar indicates the mean e-value of each set. PAAG consistently exhibits better performance on all metrics compared with other models. Fine-tuning also introduces additional improvement for PAAG.**

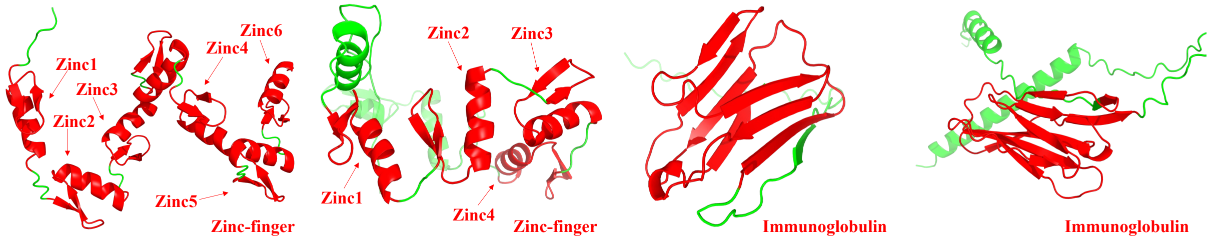

**Prompt**: From Human, contains 200 amino acids, has 8 C2H2-type Zinc finger, has 1 C2H2-type 2; degenerate Zinc finger. **E-value**: 1.8e-7

**Prompt**: From Zebrafish, contains 200 amino acids, has 11 C2H2-type Zinc finger, has 1 C2H2-type 6; degenerate Zinc finger. **E-value**: 1.8e-7

**Prompt**: From Human, contains 117 amino acids, has 1 Ig-like Immunoglobulin domain. **E-value**: 1.4e-08

**Prompt**: From Human, contains 200 amino acids, has 3 Ig-like V-type Immunoglobulin domain. **E-value**: 1.6e-08

**Figure 4: Visualization of the generated results on zinc-finger and immunoglobulin domain. The corresponding prompt and generation qualify (e-value) is listed below.**

**Model training:** We train PAAG on ProtAnnotation for total 100 epochs, employing a learning rate of 3e-5 and incorporating a warm-up phase with a batch size of 32. Additionally, we extract a subset of ProtAnnotation which only contains proteins with "zinc-finger" and "immunoglobulin domain". This subset is subsequently utilized to fine-tune the model over 5 epochs, adopting a learning rate of 1e-5 and maintaining the batch size at 32. We denote this fine-tuned version as PAAG$_{\text{ft}}$, and the PAAG without fine-tuning is denoted as PAAG. The generalization ability of PAAG$_{\text{ft}}$ is also evaluated in A.4. More details are deferred to Appendix A.7.2.

**Baselines:** We adopt ProtenDT [31], Chroma [21] and ProGen [32] as the baselines due to their public availability of model weights and their capacity to accept text and keywords as conditional inputs for protein generation. ProGen utilizes keywords as its condition tags. Here, we take the keywords correspond to zinc-finger ("KW-0863") and immunoglobulin domain ("KW-0393") in Uniport to generate functional proteins. Chroma adopts ProCap to understand the textual conditions to guide its diffusion process. We give the same text prompts to Chroma to enable its controllable generation. We also include two trivial baselines Random$_{\text{Uniform}}$ and Random$_{\text{Empirical}}$ as the blank references.

**Results:** In Figure 3 (a) and (b), we plot the curves depicting the variation in success rate SR$_e$ for different models in two protein design tasks as the quality threshold $e$ varies from 0.001 to 100. Additionally, in Figure 3 (c) and (d), we employ violin plots to illustrate the distribution of e-value $e$ for generated sequences matched in Pfam. Due to Pfam's limitations, e-values exceeding 100 are adjusted to the maximum e-value score among all method results for the current task. We also show the distribution of e-values calculated on natural proteins with domains as a reference. From Figure 3, we can observe that:

- PAAG achieves significantly higher success rates SR$_1$ across all tasks by a large margin, e.g. , 51% versus 22% in immunoglobulin domain task with quality threshold $e = 1$. Furthermore, the fine-tuned $PAAG_{ft}$ can further improve the success rates (54.3% on SR$_1$) consistently, indicating the finetuning process can help to further improve the quality.
- ProGen and ProteinDT outperform other baseline methods. This may be due to they memorizing proteins with zinc and lg domain in the training data and output them when using keywords or textual prompts.
- Chroma's performance is not good, resembles the unconditioned results. This may be because Chroma's training text primarily focuses on structural descriptions, making it less sensitive to the domain annotations.

**Visualizations:** We provide the visualization of generated proteins, folded by Omegafold [53], in Figure 4. The figure 4 highlights generated domains in red and provides textual descriptions and e-value $e$ for each sequence. We observe the generated sequences accurately produce target domains as specified in the annotation set. Interestingly, in scenarios such as two zinc finger cases, when the prompt specifies the presence of multiple zinc finger domains, PAAG generates multiple functional domains in response. However, PAAG fails to capture the precise numbers of these domains, which can be a direction for future improvement.

**Prompt**: We further investigate the relationship between the number of domains in prompts and the proteins generated by PAAG. By varying only the domain count in prompts, we generate 900

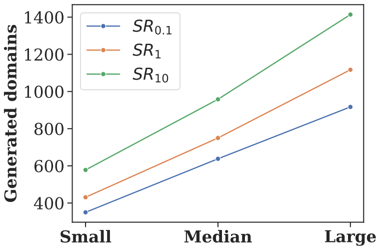

**Figure 5: The relation of number specified in prompt with generated domains by PAAG.**

proteins with 'Small (1-3)', 'Median (4-6)', and 'Large (7-9)' number of domains. Figure 5 shows that increasing domain numbers in prompts leads to a corresponding rise in generated domains across different e-values, indicating that PAAG can discern and generate the specified number of domains from text prompts through multi-level alignment. Given these observations, another interesting question is whether multiple domains in prompt will increase success rates. To this end, we re-evaluate PAAG using prompts specified only one domain ($\text{PAAG}_{\text{single domain}}$). The results are in Table 7 in Appendix. We can find while multiple domains improve success rates, $\text{PAAG}_{\text{single domain}}$ also outperforms the baselines, confirming the importance of multi-level alignment.

## 4.5 Protein Design with Property Annotations

In this section, we explore the potential of PAAG to generate proteins with certain properties guided by property annotations.

**Settings:** We employ the subcellular location of proteins as an example property. An additional dataset, termed ProtLocation, is generated by extracting subcellular location labels, encompassing Bin (2-class) task as delineated in Section 4.2, from Deeploc [3]. These labels are then incorporated into annotation-sequence pairs derived from Uniprot. ProtLocation includes 10100 proteins for training, while a separate set of 2434 test proteins is reserved for constructing the annotation set for generation. More details can be found in Appendix A.6.3.

**Evaluation protocol:** For the generated sequences, we employ the official server provided by Deeploc [3] as the pre-defined oracle to construct the Global-property metric $M_T()$ for predicting binary location label. A generation is deemed successful if the predicted label aligns with the input annotation label.

**Results:** As shown in Table 3, PAAG achieves overall 74.78% success rate, indicting PAAG captures the difference between soluble and membrane-bound, and can generate properties given corresponding property annotations. We next will move to more challenging setting, generating proteins with both domain and property annotations.

**Table 3: The result of protein design with "membrane-bound" and "soluble" annotations.**

| Annotation | Total | Matched | Success Rate |
|---|---|---|---|
| **membrane-bound** | 660 | 351 | 53.18% |
| **soluble** | 894 | 811 | 90.72% |
| **overall** | 1554 | 1162 | 74.78% |

## 4.6 Case study: Joint Generation with Domain and Property Annotations

In this part, we explore the potential of PAAG in generating proteins guided by the flexible combination of different annotations. Specifically, we generate the zinc-finger proteins in membrane-bound and soluble by the model in Section 4.5 following the same protocol in Section 4.4. Despite this challenging setting, the joint success rate $\text{SR}_1$ of generating proteins with zinc-finger and corrected property is $\text{SR}_1$ = 10.17%, However, given the current success rates of other models in generating zinc-finger proteins have approached zero, the task of producing such proteins with specific domain and property annotations remains unattainable by existing models. Zinc-finger domains are naturally occurring soluble proteins involved in DNA editing. Our generation of zinc-finger proteins anchored to the membrane underscores the efficacy of PAAG in producing novel, non-existent proteins. We showcase four examples of the generated results in Figure 6. As shown in Figure 6, PAAG can successfully generate proteins guided by both domain and property annotations, demonstrating its potential in complex protein design tasks.

## 4.7 Ablation Study

To ascertain the contribution of each component towards the generation of the functional proteins, the ablation study reports the $\text{SR}_1$ of zinc-finger and immunoglobulin domains in the absence of each alignment loss, as presented in Table 4. We observe that $\mathcal{L}_{ADC}$ is the key to the high SuccessRate of PAAG. The SuccessRate decreases to 0% without $\mathcal{L}_{ADC}$, underscoring the importance of incorporating domain range into the learning framework. Furthermore, $\mathcal{L}_{APC}$ and $\mathcal{L}_{APM}$ also enhance the SuccessRate of generating high-quality immunoglobulin domains by 4.33% and 3.33%, respectively. Moreover, $\mathcal{L}_{APC}$ and $\mathcal{L}_{APM}$ are more important to zinc-finger domain, by improving the $\text{SR}_1$ by 12% and 9.67%.

**Table 4: Ablation study for each component. Performance of $\text{SR}_1$ for zinc-finger and immunoglobulin domains.**

| $\mathcal{L}_{ADC}$ | $\mathcal{L}_{APC}$ | $\mathcal{L}_{APM}$ | Zinc-finger | Immunoglobulin |
|---|---|---|---|---|
|  | ✓ | ✓ | 0.00% | 0.33% |
| ✓ |  | ✓ | 39.00% | 18.33% |
| ✓ | ✓ |  | 41.33% | 19.33% |
| ✓ | ✓ | ✓ | **51.00%** | **22.67%** |

# 5 RELATED WORK

**Moltimodal Representation Learning.** By harnessing the potential of extensive image-text pair data, the Contrastive Language-Image Pretraining (CLIP) model, as proposed by Radford et al. [37], employs contrastive learning to align the representations between image and text modalities.Following by CLIP, many image-text pertaining model are proposed, such as BILP [26], BLIP-2 [25], InstructBLIP [10] and ClipCap [36]. Beyond the image-text pretraining, several studies introduce the more modalities, such as videos [55], audios [50] and even molecules [30, 59] into a unified representation. Specifically, for multimodal learning on protein sequences, OntoProtein [58] first learns protein representations by combining them with textual descriptions in a knowledge graph. ProtST [56] constructs a large-scale dataset containing aligned pairs of protein sequences and property descriptions, and pretrain

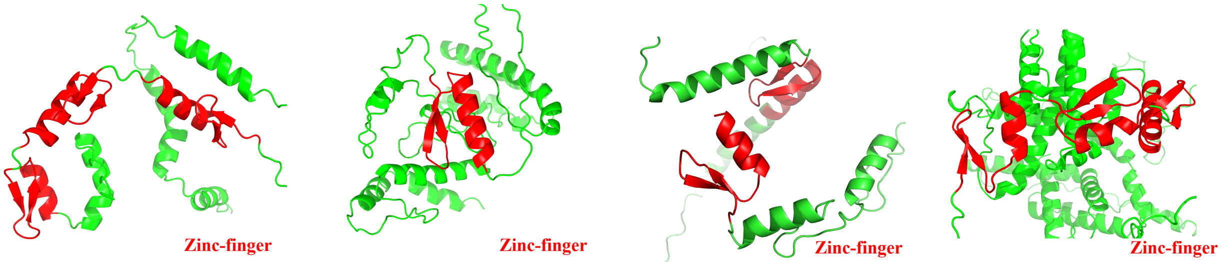

**Prompt**: From Mouse, contains 200 amino acids, has 5 C2H2-type Zinc finger, is membrane-bound.
**E-value**: 3.4e-06
**Predicted Property**: membrane-bound

**Prompt**: From Human, contains 293 amino acids, has 1 C2H2-type Zinc finger, is membrane-bound.
**E-value**: 1.6e-08
**Predicted Property**: membrane-bound

**Prompt**: From Unknown, contains 295 amino acids, has 1 C2H2-type 1; degenerate Zinc finger, has 1 C2H2-type Zinc finger, is soluble.
**E-value**: 4.2e-07
**Predicted Property**: Soluble.

**Prompt**: From Human, contains 677 amino acids, has 1 C2H2-type Zinc finger, has 1 C2H2-type 2; atypical Zinc finger, is soluble.
**E-value**: 8.7e-06
**Predicted Property**: Soluble.

**Figure 6: Visualization of jointly generation with domain and property annotations. PAAG is capable of integrating domain and property annotations.**

a protein-biotext model to improve performance on downstream predictive task and enables zero-shot retrieval.

**Protein Generation Model.** With huge success of language models [12], several studies [14, 15, 40, 43] treat protein sequences consisting chains of amino acids as a type of "languages" and pretrain models on millions of protein sequences. Upon the pretrained model, they generate the protein sequences in an autoregressive manner. In addition to the autoregressive model, Evodiff [2] extracts the evolutionary information from protein sequences and proposes an evolution-guided diffusion model to generate protein sequences. Given the significance of structural information for protein function, a group of methods [19, 20, 22, 49], known as inverse folding, utilize the structure as a conditional input, allowing for the generation of amino acid sequences. Some studies [42, 51] integrate both sequential and structural information and propose a co-design model that accepts sequences and structures as conditions. Recently, ProteinDT [31] first proposes a text-sequence alignment framework, enabling its capabilities for text-guided protein generation and editing. Chroma [21] trains a protein caption model ProCap and utilize it as a classifier guidance to generate proteins via a diffusion model.

Although ProteinDT [31] and ProtST [56] similarly align the protein and textual representations, the multi-level alignment framework enables PAAG to capture the both local and global properties of the protein. Furthermore, the momentum encoders and an additional matching loss assist PAAG to more effectively align the protein-level annotation with the proteins.

## 6 CONCLUSION

This paper presents PAAG, a multi-modality framework that first incorporates the rich annotation information derived from protein database, achieving the superior performance in various applications, such as representation learning and annotation-guided protein design. Crucially, we demonstrate that it is possible to use the flexible combinations of various kinds of textual annotations to guide the protein design process. We hope that PAAG will expand the possibilities of protein design and establish a robust foundation for future advancements in protein-related applications. Future research directions include functional protein editing, co-design of protein sequence-structure within alignment frameworks, and exploring the potential of larger protein dataset with lower annotation quality.

## ACKNOWLEDGMENTS

The authors would like to thank Siying Xu (China Academy of Art) for her help in visualizing the framework and results. This work was jointly supported by the following projects: the National Natural Science Foundation of China (No. 62376276); Beijing Nova Program (No. 20230484278); Beijing Outstanding Young Scientist Program (No. BJJWZYJH012019100020098); the Fundamental Research Funds for the Central Universities, and the Research Funds of Renmin University of China (23XNKJ19).

## REFERENCES

[1] Sarah Alamdari, Nitya Thakkar, Rianne van den Berg, Alex Xijie Lu, Nicolo Fusi, Ava Pardis Amini, and Kevin K Yang. 2023. Protein generation with evolutionary diffusion: sequence is all you need. *bioRxiv* (2023), 2023–09.

[2] Sarah Alamdari, Nitya Thakkar, Rianne van den Berg, Alex X. Lu, Nicolo Fusi, Ava P. Amini, and Kevin K. Yang. 2023. Protein generation with evolutionary diffusion: sequence is all you need. *bioRxiv* (2023). https://doi.org/10.1101/2023.09.11.556673 arXiv:https://www.biorxiv.org/content/early/2023/09/12/2023.09.11.556673.full.pdf

[3] José Juan Almagro Armenteros, Casper Kaae Sønderby, Søren Kaae Sønderby, Henrik Nielsen, and Ole Winther. 2017. DeepLoc: prediction of protein subcellular localization using deep learning. *Bioinformatics* 33, 21 (2017), 3387–3395.

[4] Miguel A Andrade, Chris P Ponting, Toby J Gibson, and Peer Bork. 2000. Homology-based method for identification of protein repeats using statistical significance estimates. *Journal of molecular biology* 298, 3 (2000), 521–537.

[5] Amos Bairoch and Rolf Apweiler. 2000. The SWISS-PROT protein sequence database and its supplement TrEMBL in 2000. *Nucleic acids research* 28, 1 (2000), 45–48.

[6] Iz Beltagy, Kyle Lo, and Arman Cohan. 2019. SciBERT: A Pretrained Language Model for Scientific Text. arXiv:1903.10676 [cs.CL]

[7] T Brummendorf. 1995. Cell adhesion molecules. 1. Immunoglobulin superfamily. *Protein profile* 2 (1995), 963–1108.

[8] Matteo Cassandri, Artem Smirnov, Flavia Novelli, Consuelo Pitolli, Massimiliano Agostini, Michal Malewicz, Gerry Melino, and Giuseppe Raschellà. 2017. Zinc-finger proteins in health and disease. *Cell death discovery* 3, 1 (2017), 1–12.

[9] The UniProt Consortium. 2022. UniProt: the Universal Protein Knowledgebase in 2023. *Nucleic Acids Research* 51, D1 (11 2022), D523–D531. https://doi.org/10.1093/nar/gkac1052 arXiv:https://academic.oup.com/nar/article-pdf/51/D1/D523/48441158/gkac1052.pdf

[10] Wenliang Dai, Junnan Li, Dongxu Li, Anthony Tiong, Junqi Zhao, Weisheng Wang, Boyang Li, Pascale Fung, and Steven Hoi. 2023. InstructBLIP: Towards General-purpose Vision-Language Models with Instruction Tuning. In *Thirty-seventh Conference on Neural Information Processing Systems*. https://openreview.net/forum?id=vvoWPYqZJA

[11] Christian Dallago, Jody Mou, Kadina E Johnston, Bruce J Wittmann, Nicholas Bhattacharya, Samuel Goldman, Ali Madani, and Kevin K Yang. 2021. FLIP: Benchmark tasks in fitness landscape inference for proteins. *bioRxiv* (2021), 2021–11.

[12] Jacob Devlin, Ming-Wei Chang, Kenton Lee, and Kristina Toutanova. 2019. BERT: Pre-training of Deep Bidirectional Transformers for Language Understanding. arXiv:1810.04805 [cs.CL]

[13] J Drenth, JN Jansonius, R Koekoek, HM Swen, and BG Wolthers. 1968. Structure of papain. *Nature* 218, 5145 (1968), 929–932.

[14] Ahmed Elnaggar, Michael Heinzinger, Christian Dallago, Ghalia Rehawi, Wang Yu, Llion Jones, Tom Gibbs, Tamas Feher, Christoph Angerer, Martin Steinegger, Debsindhu Bhowmik, and Burkhard Rost. 2021. ProtTrans: Towards Cracking the Language of Lifes Code Through Self-Supervised Deep Learning and High Performance Computing. *IEEE Transactions on Pattern Analysis and Machine Intelligence* (2021), 1–1. https://doi.org/10.1109/TPAMI.2021.3095381

[15] Noelia Ferruz, Steffen Schmidt, and Birte Höcker. 2022. ProtGPT2 is a deep unsupervised language model for protein design. *Nature communications* 13, 1 (2022), 4348.

[16] Yaron Geffen, Yanay Ofran, and Ron Unger. 2022. DistilProtBert: a distilled protein language model used to distinguish between real proteins and their randomly shuffled counterparts. *Bioinformatics* 38, Supplement_2 (2022), ii95–ii98.

[17] Kaiming He, Haoqi Fan, Yuxin Wu, Saining Xie, and Ross Girshick. 2020. Momentum contrast for unsupervised visual representation learning. In *Proceedings of the IEEE/CVF conference on computer vision and pattern recognition.* 9729–9738.

[18] KN Houk, Andrew G Leach, Susanna P Kim, and Xiyun Zhang. 2003. Binding affinities of host–guest, protein–ligand, and protein–transition-state complexes. *Angewandte Chemie International Edition* 42, 40 (2003), 4872–4897.

[19] Chloe Hsu, Robert Verkuil, Jason Liu, Zeming Lin, Brian Hie, Tom Sercu, Adam Lerer, and Alexander Rives. 2022. Learning inverse folding from millions of predicted structures. In *International Conference on Machine Learning*. PMLR, 8946–8970.

[20] John Ingraham, Vikas Garg, Regina Barzilay, and Tommi Jaakkola. 2019. Generative models for graph-based protein design. *Advances in neural information processing systems* 32 (2019).

[21] John B Ingraham, Max Baranov, Zak Costello, Karl W Barber, Wujie Wang, Ahmed Ismail, Vincent Frappier, Dana M Lord, Christopher Ng-Thow-Hing, Erik R Van Vlack, et al. 2023. Illuminating protein space with a programmable generative model. *Nature* 623, 7989 (2023), 1070–1078.

[22] Bowen Jing, Stephan Eismann, Patricia Suriana, Raphael JL Townshend, and Ron Dror. 2020. Learning from protein structure with geometric vector perceptrons. *arXiv preprint arXiv:2009.01411* (2020).

[23] A Klug and D Rhodes. 1987. Zinc fingers: a novel protein fold for nucleic acid recognition. In *Cold Spring Harbor symposia on quantitative biology*, Vol. 52. Cold Spring Harbor Laboratory Press, 473–482.

[24] Jiwei Li, Michel Galley, Chris Brockett, Jianfeng Gao, and Bill Dolan. 2016. A Diversity-Promoting Objective Function for Neural Conversation Models. In *Proceedings of the 2016 Conference of the North American Chapter of the Association for Computational Linguistics: Human Language Technologies*, Kevin Knight, Ani Nenkova, and Owen Rambow (Eds.). Association for Computational Linguistics, San Diego, California, 110–119. https://doi.org/10.18653/v1/N16-1014

[25] Junnan Li, Dongxu Li, Silvio Savarese, and Steven Hoi. 2023. Blip-2: Bootstrapping language-image pre-training with frozen image encoders and large language models. *arXiv preprint arXiv:2301.12597* (2023).

[26] Junnan Li, Dongxu Li, Caiming Xiong, and Steven Hoi. 2022. BLIP: Bootstrapping Language-Image Pre-training for Unified Vision-Language Understanding and Generation. In *ICML*.

[27] Junnan Li, Ramprasaath Selvaraju, Akhilesh Gotmare, Shafiq Joty, Caiming Xiong, and Steven Chu Hong Hoi. 2021. Align before fuse: Vision and language representation learning with momentum distillation. *Advances in neural information processing systems* 34 (2021), 9694–9705.

[28] Zeming Lin, Halil Akin, Roshan Rao, Brian Hie, Zhongkai Zhu, Wenting Lu, Nikita Smetanin, Robert Verkuil, Ori Kabeli, Yaniv Shmueli, et al. 2023. Evolutionary-scale prediction of atomic-level protein structure with a language model. *Science* 379, 6637 (2023), 1123–1130.

[29] Shengchao Liu, Yanjing Li, Zhuoxinran Li, Anthony Gitter, Yutao Zhu, Jiarui Lu, Zhao Xu, Weili Nie, Arvind Ramanathan, Chaowei Xiao, Jian Tang, Hongyu Guo, and Anima Anandkumar. 2023. A Text-guided Protein Design Framework. arXiv:2302.04611 [cs.LG]

[30] Shengchao Liu, Weili Nie, Chengpeng Wang, Jiarui Lu, Zhuoran Qiao, Ling Liu, Jian Tang, Chaowei Xiao, and Anima Anandkumar. 2022. Multi-modal molecule structure-text model for text-based retrieval and editing. *arXiv preprint arXiv:2212.10789* (2022).

[31] Shengchao Liu, Yutao Zhu, Jiarui Lu, Zhao Xu, Weili Nie, Anthony Gitter, Chaowei Xiao, Jian Tang, Hongyu Guo, and Anima Anandkumar. 2023. A text-guided protein design framework. *arXiv preprint arXiv:2302.04611* (2023).

[32] Ali Madani, Ben Krause, Eric R Greene, Subu Subramanian, Benjamin P Mohr, James M Holton, Jose Luis Olmos, Caiming Xiong, Zachary Z Sun, Richard Socher, et al. 2023. Large language models generate functional protein sequences across diverse families. *Nature Biotechnology* 41, 8 (2023), 1099–1106.

[33] Liam R Marshall, Oleksii Zozulia, Zsofia Lengyel-Zhand, and Ivan V Korendovych. 2019. Minimalist de novo design of protein catalysts. *ACS catalysis* 9, 10 (2019), 9265–9275.

[34] Jaina Mistry, Sara Chuguransky, Lowri Williams, Matloob Qureshi, Gustavo A Salazar, Erik LL Sonnhammer, Silvio CE Tosatto, Lisanna Paladin, Shriya Raj, Lorna J Richardson, et al. 2021. Pfam: The protein families database in 2021. *Nucleic acids research* 49, D1 (2021), D412–D419.

[35] T.K. Mohandas, X.-N. Chen, L.B. Rowe, E.H. Birkenmeier, A.S. Fanning, J.M. Anderson, and J.R. Korenberg. 1995. Localization of the Tight Junction Protein Gene TJP1 to Human Chromosome 15q13, Distal to the Prader-Willi/Angelman Region, and to Mouse Chromosome 7. *Genomics* 30, 3 (1995), 594–597. https://doi.org/10.1006/geno.1995.1281

[36] Ron Mokady, Amir Hertz, and Amit H Bermano. 2021. Clipcap: Clip prefix for image captioning. *arXiv preprint arXiv:2111.09734* (2021).

[37] Alec Radford, Jong Wook Kim, Chris Hallacy, Aditya Ramesh, Gabriel Goh, Sandhini Agarwal, Girish Sastry, Amanda Askell, Pamela Mishkin, Jack Clark, Gretchen Krueger, and Ilya Sutskever. 2021. Learning Transferable Visual Models From Natural Language Supervision. In *Proceedings of the 38th International Conference on Machine Learning (Proceedings of Machine Learning Research, Vol. 139)*, Marina Meila and Tong Zhang (Eds.). PMLR, 8748–8763. https://proceedings.mlr.press/v139/radford21a.html

[38] Roshan Rao, Nicholas Bhattacharya, Neil Thomas, Yan Duan, Peter Chen, John Canny, Pieter Abbeel, and Yun Song. 2019. Evaluating protein transfer learning with TAPE. *Advances in neural information processing systems* 32 (2019).

[39] Lynne Regan. 1995. Protein design: novel metal-binding sites. *Trends in biochemical sciences* 20, 7 (1995), 280–285.

[40] Alexander Rives, Joshua Meier, Tom Sercu, Siddharth Goyal, Zeming Lin, Jason Liu, Demi Guo, Myle Ott, C. Lawrence Zitnick, Jerry Ma, and Rob Fergus. 2019. Biological Structure and Function Emerge from Scaling Unsupervised Learning to 250 Million Protein Sequences. *PNAS* (2019). https://doi.org/10.1101/622803

[41] Amir Shanehsazzadeh, David Belanger, and David Dohan. 2020. Is transfer learning necessary for protein landscape prediction? *arXiv preprint arXiv:2011.03443* (2020).

[42] Chence Shi, Chuanrui Wang, Jiarui Lu, Bozitao Zhong, and Jian Tang. 2022. Protein sequence and structure co-design with equivariant translation. *arXiv preprint arXiv:2210.08761* (2022).

[43] Jung-Eun Shin, Adam J Riesselman, Aaron W Kollasch, Conor McMahon, Elana Simon, Chris Sander, Aashish Manglik, Andrew C Kruse, and Debora S Marks. 2021. Protein design and variant prediction using autoregressive generative models. *Nature communications* 12, 1 (2021), 2403.

[44] Gregory Sliwoski, Sandeepkumar Kothiwale, Jens Meiler, and Edward W Lowe. 2014. Computational methods in drug discovery. *Pharmacological reviews* 66, 1 (2014), 334–395.

[45] Dean G Stathakis, Kevin B Hoover, Zhiyong You, and Peter J Bryant. 1997. Human postsynaptic density-95 (PSD95): location of the gene (DLG4) and possible function in nonneural as well as in neural tissues. *Genomics* 44, 1 (1997), 71–82.

[46] Martin Steinegger and Johannes Söding. 2017. MMseqs2 enables sensitive protein sequence searching for the analysis of massive data sets. *Nature biotechnology* 35, 11 (2017), 1026–1028.

[47] Reinhard Sterner, Rainer Merkl, and Frank M. Raushel. 2008. Computational Design of Enzymes. *Chemistry & Biology* 15, 5 (2008), 421–423. https://doi.org/10.1016/j.chembiol.2008.04.007

[48] Melody A Swartz, Sachiko Hirosue, and Jeffrey A Hubbell. 2012. Engineering approaches to immunotherapy. *Science translational medicine* 4, 148 (2012), 148rv9–148rv9.

[49] Cheng Tan, Zhangyang Gao, Jun Xia, Bozhen Hu, and Stan Z Li. 2022. Generative de novo protein design with global context. *arXiv preprint arXiv:2204.10673* (2022).

[50] Zineng Tang, Ziyi Yang, Chenguang Zhu, Michael Zeng, and Mohit Bansal. 2023. Any-to-Any Generation via Composable Diffusion. *arXiv preprint arXiv:2305.11846* (2023).

[51] Joseph L Watson, David Juergens, Nathaniel R Bennett, Brian L Trippe, Jason Yim, Helen E Eisenach, Woody Ahern, Andrew J Borst, Robert J Ragotte, Lukas F Milles, et al. 2023. De novo design of protein structure and function with RFdiffusion. *Nature* 620, 7976 (2023), 1089–1100.

[52] Fandi Wu, Yu Zhao, Jiaxiang Wu, Biaobin Jiang, Bing He, Longkai Huang, Chenchen Qin, Fan Yang, Ningqiao Huang, Yang Xiao, et al. 2024. Fast and accurate modeling and design of antibody-antigen complex using tFold. *bioRxiv* (2024), 2024–02.

[53] Ruidong Wu, Fan Ding, Rui Wang, Rui Shen, Xiwen Zhang, Shitong Luo, Chenpeng Su, Zuofan Wu, Qi Xie, Bonnie Berger, et al. 2022. High-resolution de novo structure prediction from primary sequence. *BioRxiv* (2022), 2022–07.

[54] Zhirong Wu, Yuanjun Xiong, X Yu Stella, and Dahua Lin. 2018. Unsupervised Feature Learning via Non-Parametric Instance Discrimination. In *Proceedings of the IEEE Conference on Computer Vision and Pattern Recognition.*

[55] Hu Xu, Gargi Ghosh, Po-Yao Huang, Dmytro Okhonko, Armen Aghajanyan, Florian Metze, Luke Zettlemoyer, and Christoph Feichtenhofer. 2021. VideoCLIP: Contrastive Pre-training for Zero-shot Video-Text Understanding. *CoRR* abs/2109.14084 (2021). arXiv:2109.14084 https://arxiv.org/abs/2109.14084

[56] Minghao Xu, Xinyuan Yuan, Santiago Miret, and Jian Tang. 2023. ProtST: Multi-Modality Learning of Protein Sequences and Biomedical Texts. *arXiv preprint arXiv:2301.12040* (2023).

[57] Minghao Xu, Zuobai Zhang, Jiarui Lu, Zhaocheng Zhu, Yangtian Zhang, Ma Chang, Runcheng Liu, and Jian Tang. 2022. Peer: a comprehensive and multi-task benchmark for protein sequence understanding. *Advances in Neural Information*

*Processing Systems* 35 (2022), 35156–35173.

[58] Ningyu Zhang, Zhen Bi, Xiaozhuan Liang, Siyuan Cheng, Haosen Hong, Shumin Deng, Jiazhang Lian, Qiang Zhang, and Huajun Chen. 2022. OntoProtein: Protein Pretraining With Gene Ontology Embedding. arXiv:2201.11147 [q-bio.BM]

[59] Yikun Zhang, Geyan Ye, Chaohao Yuan, Bo Han, Long-Kai Huang, Jianhua Yao, Wei Liu, and Yu Rong. 2024. Atomas: Hierarchical Alignment on Molecule-Text for Unified Molecule Understanding and Generation. *arXiv preprint arXiv:2404.16880* (2024).

[60] Kangfei Zhao, Yu Rong, Biaobin Jiang, Jianheng Tang, Hengtong Zhang, Jeffrey Xu Yu, and Peilin Zhao. 2023. Geometric Graph Learning for Protein Mutation Effect Prediction. In *Proceedings of the 32nd ACM International Conference on Information and Knowledge Management.* 3412–3422.

# A EXPERIMENTAL SETTINGS

## A.1 General settings

**Backbone Models of PAAG:** We use ProtBert-BFD [14] to initialize our protein encoder and SciBert [6] for the text encoder. Due to limited training data, we opt for a lighter decoder initialized by DistilProtBert [16]. Exploring a decoder with more parameters is a future direction.

**Training Configurations:** We train PAAG on ProtAnnotation, using the AdamW optimizer (with a learning rate of 3e-5 and zero weight decay) for 100 epochs. Our generation experiments are conducted on 16 NVIDIA Tesla A100-SX4-40GB GPUs.

## A.2 ProtAnnotation and template function $G(\cdot)$

Table 5 depicts additional statistics of ProtAnnotation. We demonstrate several example data samples in ProtAnnotation as well as the corresponding textual description generated by the template function $G(\cdot)$.

**Table 5: The statistics of ProtAnnotation**

| # of proteins | # of distinct domains | average # of domains per protein | average length |
|---|---|---|---|
| 129,727 | 1,416 | 1.60 | 419.40 |

The explanation of four property annotations:

- **protein_name**: The protein name is a naming method used to describe the function, characteristics, or origin of a protein. These names usually contain information about the protein's structure, function, substrate specificity, and biological process.
- **organism_name**: Organism names are used to identify and classify different species of living organisms, including bacteria, fungi, plants, and animals. These names usually consist of the genus and species of the organism, and sometimes include additional information such as strain or cultivar.
- **length**: The number of amino acids in the protein sequence.
- **SIMILARITY**: In the context of biology and protein classification, "similarity" refers to the shared characteristics or features among different proteins. This can include similar structures, functions, or evolutionary origins. Proteins with high similarity are often grouped into the same family or subfamily.

## A.3 Biological background of zinc-finger and immunoglobulin domain

We here introduce zinc-finger and immunoglobulin domains, highlighting their biological significance and functions in biology.

- **Zinc-finger:** Zinc finger [23] domains are compact protein motifs known for binding DNA, RNA, proteins, and lipids, with binding characteristics influenced by amino acid sequence, linker structure, and number of fingers. Despite appearing in various protein families, they maintain stable structures and are crucial in processes like gene transcription and mRNA trafficking.
- **Immunoglobulin domain:** Immunoglobulin (Ig) domains play a key role in protein-protein interactions, especially within the immune system, where they help recognize, bind, and neutralize antigens. These domains have a conserved structure found in a variety of proteins, including antibodies and cell adhesion molecules.

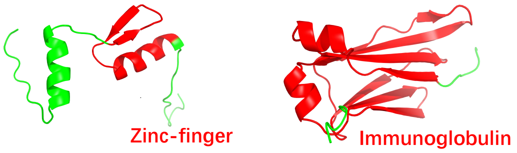

**Figure 7: Visualization of typical proteins containing Zinc-finger (P26634) and Immunoglobulin (A0M8Q6).**

Examples of Zinc-finger and Ig domains are shown in Figure 7.

## A.4 The evaluation metric for the unconditional generation

In the computation of the Distinct-n metric, we assign a value of $n$ to 2. For the Novelty metric, the default parameters of Mmseq2 are employed with an exception for the e-value threshold, which is designated as 100. In the case of the Diversity metric, the default parameters of Mmseq2 are again utilized, but with alterations to the e-value threshold and sensitivity, set to 1000000 and 15 respectively. During the application of Mmseq2 for the calculation of Novelty and Diversity metrics, the dissimilarity for unmatched sequences is assumed to be 1.0.

## A.5 More details of baselines

ProGen [32] represents each protein property as keyword tags, which are prepended to amino acid sequences during training to enable auto-regressive reconstruction. This allows ProGen to generate protein sequences from keyword tags. For controllable generation, ProGen translates desired properties into keyword tags to guide sequence generation.

Chroma [21] is a protein design model focusing on generating protein backbones. It uses classifier guidance and ProCap, a protein-to-text model, for text-guided designs. With a sequence sampling model, Chroma can generate both structure and sequence based on specified conditions.

ProteinDT [31] is a text-guided protein design model that aligns protein and text representations, then uses aligned text representations to design protein sequences via autoregressive and diffusion models. For fair comparison, we use autoregressive ProteinDT as our baseline. In unconditional generation, due to the lack of a specific template in ProteinDT, we randomly sample prompts from its dataset to evaluate the quality of generated proteins. In conditional experiments, ProteinDT receives the same prompts as PAAG.

In unconditional generation, PAAG accepts only the protein sequence length $l$ and the order $k$ of protein generated, using the template: "protein number k, contains l amino acids." For generating proteins with functional domains, we randomly sample organism names, lengths, and similarities from natural proteins with the corresponding domains. Generative hyper-parameters are specified

**Table 6: Examples of annotations and description of protein in ProtAnnotation**

| Entry name | Domain Annotation | Property Annotation | Textual Description G(D) |
|---|---|---|---|
| Q8W4R8 | [38, 95], Ubiquitin-like; degenerate domain<br>[158, 459],PI3K/PI4K catalytic domain | **organism_name**: Mouse-ear cress,<br>**protein_name**: Phosphatidylinositol 4-kinase gamma 6,<br>**length**: 622,<br>**SIMILARITY**: Belongs to the PI3/PI4-kinase family, Type II PI4K subfamily | This is Phosphatidylinositol 4-kinase gamma 6 protein, from Mouse-ear cress, belongs to the PI3/PI4-kinase family, Type II PI4K subfamily, contains 622 amino acids, has 1 Ubiquitin-like; degenerate domain, has 1 PI3K/PI4K catalytic domain. |
| Q8XAW7 | [5, 241], ABC transporter domain<br>[252, 495], ABC transporter domain | **organism_name**: Escherichia coli O157:H7,<br>**protein_name**: Ribose import ATP-binding protein RbsA 1,<br>**length**: 501,<br>**SIMILARITY**: Belongs to the ABC transporter superfamily, Ribose importer (TC 3,A,1,2,1) family | This is Ribose import ATP-binding protein RbsA 1 protein, from Escherichia coli O157:H7, belongs to the ABC transporter superfamily, Ribose importer (TC 3,A,1,2,1) family, contains 501 amino acids, has 2 ABC transporter domain. |

in A.6. Using property annotations, we apply the template function $G()$ to describe test data from the Deeploc [3] dataset, enabling PAAG to generate proteins with specified properties.

## A.6 Training configurations

*A.6.1 Predictive Task.* In downstream prediction tasks, PAAG uses embeddings in the aligned space by employing both the protein encoder and the projector head for more informative aligned features. Hyperparameters for predictive tasks using PAAG-ProtBert and PAAG-ESM-2 are detailed in Table 9 and Table 10.

*A.6.2 Protein Design with Domain Annotations.* While training PAAG with ProtAnnotation, we incorporate momentum contrast [17] with a queue size of 16,384 and momentum of 0.995. The learnable temperature in contrastive learning is set to 0.07, and our latent space is aligned to 256 dimensions with a linear layer. Following [26], we initialize learnable alpha at 0.4 for soft labeling. When fine-tuning on datasets with only zinc-finger and immunoglobulin domains, we maintain these hyperparameters but reduce the queue size to 4,096 due to less training data. Additionally, weight decay for AdamW is set at 0.05.

In our generative task, we use nucleus sampling in the decoder, sampling amino acids based on probability rather than always selecting the highest probability ones. The Top-p hyperparameter is set to 0.9, meaning the decoder considers the top 90% probability mass. We also set the decoder's repetition penalty to 1.2.

*A.6.3 Protein Design with Property Annotations.* Due to limited training data, we fine-tune the models from Section 4.4 for 100 epochs. We retain the ProtAnnotation training hyperparameters but lower the learning rate to 1e-5 without warm-up.

For binary localization properties, soluble and membrane-bound, we set template function $G()$ as "is soluble" or "is membrane-bound".

## A.7 Additional experimental results

*A.7.1 Results of generating proteins with EGF-like domain.* We here generates 300 functional proteins with EGF-like domain for ProGen, ProteinDT and PAAG. The results are in Table 11.

**Table 7: The success rate on the prompt with single domain.**

| Method | $SR_1$(Zinc finger) | $SR_1$(Immunoglobulin) |
|---|---|---|
| **Chroma** | 0.33% | 0% |
| **ProteinDT** | 1.67% | 22% |
| **PAAG** | 22.67% | 51% |
| **$PAAG_{single domain}$** | 18.33% | 46% |

**Table 8: Results of the proteins unconditionally generated by fine-tuned PAAG.**

| Model | Distinc-2 | Diversity | Novelty |
|---|---|---|---|
| **Natural** | 0.4309(0) | 0.829(0) | - |
| **ProGen** | 0.3003(30.31%) | 0.845(1.93%) | 0.374 |
| **Chroma** | 0.3211(25.48%) | 0.855(3.14%) | 0.638 |
| **$PAAG_{before ft}$** | 0.4314(0.12%) | 0.815(1.69%) | 0.766 |
| **$PAAG_{after ft}$** | 0.4524(4.99%) | 0.822(0.84%) | 0.674 |

**Table 9: Configurations of full-model tuning of PAAG-ProtBert. *Abbr.*, lr.: learning rate; lrr.: learning rate ratio; dr.: dropout rate; wd.: weight decay; bs.: batch size; MSE: mean squared error; CE: cross entropy; BCE: binary cross entropy.**

| Task | lr. | lrr. | dr. | wd. | bs. | #epochs | loss |
|---|---|---|---|---|---|---|---|
| | | | **Localization** | | | | |
| **Bin** | $2.0 \times 10^{-5}$ | 0.15 | 0 | 0 | 4 | 100 | BCE |
| **Sub** | $2.0 \times 10^{-5}$ | 0.15 | 0.1 | 0 | 4 | 100 | CE |
| | | | **Fitness** | | | | |
| **$\rho$-lac** | $2.0 \times 10^{-4}$ | 0.02 | 0 | $3.0 \times 10^{-4}$ | 36 | 100 | MSE |
| **AAV** | $9.0 \times 10^{-4}$ | 0.02 | 0 | 0 | 36 | 100 | MSE |
| **Thermo** | $2.0 \times 10^{-4}$ | 0.02 | 0 | 0 | 6 | 100 | MSE |
| **Flu** | $2.0 \times 10^{-4}$ | 0.02 | 0.3 | $4.0 \times 10^{-4}$ | 36 | 100 | MSE |
| **Sta** | $5.0 \times 10^{-4}$ | 0.02 | 0.7 | 0 | 36 | 100 | MSE |

**Table 10: Hyperparameters for PAAG-ESM-2 in downstream tasks.**

| Task | lr. | lrr. | dr. | wd. | bs. | #epochs | loss |
|---|---|---|---|---|---|---|---|
| | | | **Localization** | | | | |
| **Bin** | $1.0 \times 10^{-5}$ | 0.15 | 0 | 0 | 4 | 100 | BCE |
| **Sub** | $2.0 \times 10^{-5}$ | 0.15 | 0 | 0 | 4 | 100 | CE |
| | | | **Fitness** | | | | |
| **$\rho$-lac** | $1.0 \times 10^{-4}$ | 0.02 | 0 | 0 | 16 | 100 | MSE |
| **AAV** | $8.0 \times 10^{-4}$ | 0.02 | 0 | 0 | 16 | 100 | MSE |
| **Thermo** | $3.0 \times 10^{-4}$ | 0.02 | 0.6 | 0 | 2 | 100 | MSE |
| **Flu** | $3.0 \times 10^{-4}$ | 0.02 | 0 | 0 | 16 | 100 | MSE |
| **Sta** | $8.0 \times 10^{-5}$ | 0.02 | 0 | 0 | 16 | 100 | MSE |

**Table 11: Success Rate of generating proteins with EGF-like domain.**

| EFG-like domain | $SR_{100}$ | $SR_{10}$ | $SR_1$ | $SR_{0.1}$ | $SR_{0.01}$ | $SR_{0.001}$ |
|---|---|---|---|---|---|---|
| **ProGen** | 1% | 1% | 1% | 1% | 1% | 1% |
| **ProteinDT** | 0% | 0% | 0% | 0% | 0% | 0% |
| **PAAG** | **28.67%** | **28.33%** | **26.00%** | **22.33%** | **17.33%** | **11.67%** |

*A.7.2 More evaluation on the proteins generated by fine-tuned PAAG.* To ensure fine-tuned PAAG isn't just memorizing the training set, we evaluate distinct-2, diversity, and novelty for unconditionally generated sequences. Table 8 shows that, even after fine-tuning, PAAG produces proteins with higher novelty than Chroma and ProGen, indicating it doesn't overfit, thanks to label smoothing. Additionally, fine-tuned PAAG's diversity is closest to natural proteins, suggesting it captures similar amino acid distributions.